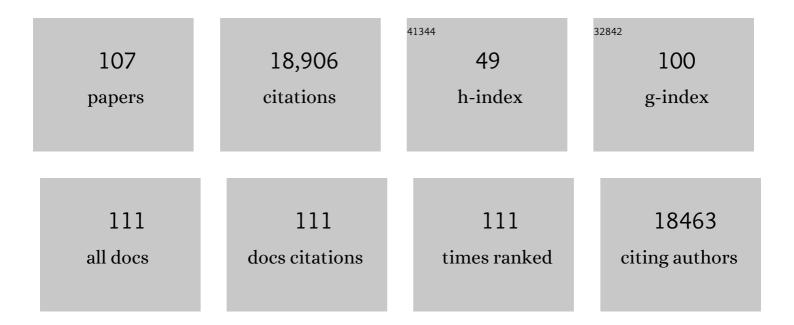
Zhengguo Xiao

List of Publications by Year in descending order

Source: https://exaly.com/author-pdf/787707/publications.pdf Version: 2024-02-01



#	Article	IF	CITATIONS
1	Alkalis-doping of mixed tin-lead perovskites for efficient near-infrared light-emitting diodes. Science Bulletin, 2022, 67, 54-60.	9.0	13
2	Guanidinium-assisted crystallization modulation and reduction of open-circuit voltage deficit for efficient planar FAPbBr3 perovskite solar cells. Chemical Engineering Journal, 2022, 437, 135181.	12.7	15
3	Largeâ€Area and Efficient Skyâ€Blue Perovskite Lightâ€Emitting Diodes via Blade oating. Advanced Materials, 2022, 34, e2108939.	21.0	20
4	A Selective Targeting Anchor Strategy Affords Efficient and Stable Idealâ€Bandgap Perovskite Solar Cells. Advanced Materials, 2022, 34, e2110241.	21.0	44
5	High Radiance of Perovskite Lightâ€Emitting Diodes Enabled by Perovskite Heterojunctions. Advanced Functional Materials, 2022, 32, .	14.9	11
6	Trade-off between the Performance and Stability of Perovskite Light-Emitting Diodes with Excess Halides. Journal of Physical Chemistry Letters, 2022, 13, 5179-5185.	4.6	2
7	Synergistic Activation of Bovine CD4+ T Cells by Neutrophils and IL-12. Pathogens, 2021, 10, 694.	2.8	4
8	Overcoming Outcoupling Limit in Perovskite Light-Emitting Diodes with Enhanced Photon Recycling. Nano Letters, 2021, 21, 8426-8432.	9.1	9
9	Polymerized Hybrid Perovskites with Enhanced Stability, Flexibility, and Lattice Rigidity. Advanced Materials, 2021, 33, e2104842.	21.0	45
10	Large-area and efficient perovskite light-emitting diodes via low-temperature blade-coating. Nature Communications, 2021, 12, 147.	12.8	100
11	Effects of Fluorination on Fused Ring Electron Acceptor for Active Layer Morphology, Exciton Dissociation, and Charge Recombination in Organic Solar Cells. ACS Applied Materials & amp; Interfaces, 2020, 12, 56231-56239.	8.0	15
12	An Electrically Modulated Singleâ€Color/Dualâ€Color Imaging Photodetector. Advanced Materials, 2020, 32, e1907257.	21.0	145
13	Efficient All-Inorganic Perovskite Light-Emitting Diodes with Improved Operation Stability. ACS Applied Materials & Interfaces, 2020, 12, 18084-18090.	8.0	54
14	Progress of the key materials for organic solar cells. Science China Chemistry, 2020, 63, 758-765.	8.2	158
15	Dual Passivation of Perovskite Defects for Lightâ€Emitting Diodes with External Quantum Efficiency Exceeding 20%. Advanced Functional Materials, 2020, 30, 1909754.	14.9	212
16	Simple organic donors based on halogenated oligothiophenes for all small molecule solar cells with efficiency over 11%. Journal of Materials Chemistry A, 2020, 8, 5843-5847.	10.3	43
17	CTL-Derived Exosomes Enhance the Activation of CTLs Stimulated by Low-Affinity Peptides. Frontiers in Immunology, 2019, 10, 1274.	4.8	36
18	Suppression and Reversion of Light-Induced Phase Separation in Mixed-Halide Perovskites by Oxygen Passivation. ACS Energy Letters, 2019, 4, 2052-2058.	17.4	54

#	Article	IF	CITATIONS
19	Widely Tunable, Room Temperature, Single-Mode Lasing Operation from Mixed-Halide Perovskite Thin Films. ACS Photonics, 2019, 6, 3331-3337.	6.6	31
20	Engineering Perovskite Nanocrystal Surface Termination for Lightâ€Emitting Diodes with External Quantum Efficiency Exceeding 15%. Advanced Functional Materials, 2019, 29, 1807284.	14.9	80
21	Nitrogenâ€Doped Nickel Oxide as Hole Transport Layer for Highâ€Efficiency Inverted Planar Perovskite Solar Cells. Solar Rrl, 2019, 3, 1900164.	5.8	29
22	Zwitterion Coordination Induced Highly Orientational Order of CH ₃ NH ₃ Pbl ₃ Perovskite Film Delivers a High Open Circuit Voltage Exceeding 1.2 V. Advanced Functional Materials, 2019, 29, 1901026.	14.9	134
23	Characterization of IL-10-producing neutrophils in cattle infected with Ostertagia ostertagi. Scientific Reports, 2019, 9, 20292.	3.3	12
24	Mixed Lead–Tin Halide Perovskites for Efficient and Wavelengthâ€Tunable Nearâ€Infrared Lightâ€Emitting Diodes. Advanced Materials, 2019, 31, e1806105.	21.0	66
25	Bovine neutrophils form extracellular traps in response to the gastrointestinal parasite Ostertagia ostertagi. Scientific Reports, 2018, 8, 17598.	3.3	30
26	Efficient Perovskite Solar Cells with Titanium Cathode Interlayer (Solar RRL 11â^•2018). Solar Rrl, 2018, 2, 1870226.	5.8	1
27	18â€1: Invited Paper: Color Tunable, Flexible, and Efficient Light Emitting Diodes Composed of Metal Halide Perovskites. Digest of Technical Papers SID International Symposium, 2018, 49, 212-213.	0.3	1
28	Efficient Perovskite Solar Cells with Titanium Cathode Interlayer. Solar Rrl, 2018, 2, 1800167.	5.8	16
29	Efficient perovskite light-emitting diodes featuring nanometre-sized crystallites. Nature Photonics, 2017, 11, 108-115.	31.4	1,175
30	Characterization of Ostertagia ostertagi annexin-like proteins at different developmental stages. Parasitology Research, 2017, 116, 1515-1522.	1.6	1
31	Effector functions of memory CTLs can be affected by signals received during reactivation. Immunologic Research, 2017, 65, 841-852.	2.9	4
32	<i>In Situ</i> Preparation of Metal Halide Perovskite Nanocrystal Thin Films for Improved Light-Emitting Devices. ACS Nano, 2017, 11, 3957-3964.	14.6	151
33	Mixed-Halide Perovskites with Stabilized Bandgaps. Nano Letters, 2017, 17, 6863-6869.	9.1	165
34	IL-12 stimulates CTLs to secrete exosomes capable of activating bystander CD8+ T cells. Scientific Reports, 2017, 7, 13365.	3.3	53
35	Efficient Perovskite LEDs Featuring Nanometer Sized Crystallites. , 2017, , .		0
36	Metal Halide Perovskites: Processing, Interfaces, and Light Emitting Devices. , 2017, , .		0

Metal Halide Perovskites: Processing, Interfaces, and Light Emitting Devices. , 2017, , . 36

#	Article	IF	CITATIONS
37	Ultrasmooth metal halide perovskite thin films via sol–gel processing. Journal of Materials Chemistry A, 2016, 4, 8308-8315.	10.3	64
38	Abomasal mucosal immune responses of cattle with limited or continuous exposure to pasture-borne gastrointestinal nematode parasite infection. Veterinary Parasitology, 2016, 229, 118-125.	1.8	8
39	Redox Chemistry Dominates the Degradation and Decomposition of Metal Halide Perovskite Optoelectronic Devices. ACS Energy Letters, 2016, 1, 595-602.	17.4	196
40	Transient exposure to proteins SOX2, Oct-4, and NANOG immortalizes exhausted tumor-infiltrating CTLs. Biochemical and Biophysical Research Communications, 2016, 473, 1255-1260.	2.1	0
41	Energyâ€Efficient Hybrid Perovskite Memristors and Synaptic Devices. Advanced Electronic Materials, 2016, 2, 1600100.	5.1	323
42	Unraveling the hidden function of a stabilizer in a precursor in improving hybrid perovskite film morphology for high efficiency solar cells. Energy and Environmental Science, 2016, 9, 867-872.	30.8	62
43	Thin-film semiconductor perspective of organometal trihalide perovskite materials for high-efficiency solar cells. Materials Science and Engineering Reports, 2016, 101, 1-38.	31.8	117
44	Unlocking Efficient Perovskite-based Light Emitting Devices. , 2016, , .		0
45	Unlocking Efficient Perovskite-based Light Emitting Devices. , 2016, , .		0
46	Photovoltaic Switching Mechanism in Lateral Structure Hybrid Perovskite Solar Cells. Advanced Energy Materials, 2015, 5, 1500615.	19.5	567
47	Lightâ€Induced Selfâ€Poling Effect on Organometal Trihalide Perovskite Solar Cells for Increased Device Efficiency and Stability. Advanced Energy Materials, 2015, 5, 1500721.	19.5	214
48	Improving the sensitivity of a near-infrared nanocomposite photodetector by enhancing trap induced hole injection. Applied Physics Letters, 2015, 106, .	3.3	43
49	Highâ€Gain and Lowâ€Drivingâ€Voltage Photodetectors Based on Organolead Triiodide Perovskites. Advanced Materials, 2015, 27, 1912-1918.	21.0	560
50	Distinct Exciton Dissociation Behavior of Organolead Trihalide Perovskite and Excitonic Semiconductors Studied in the Same System. Small, 2015, 11, 2164-2169.	10.0	78
51	Photodetectors: High-Gain and Low-Driving-Voltage Photodetectors Based on Organolead Triiodide Perovskites (Adv. Mater. 11/2015). Advanced Materials, 2015, 27, 1967-1967.	21.0	3
52	Non-wetting surface-driven high-aspect-ratio crystalline grain growth for efficient hybrid perovskite solar cells. Nature Communications, 2015, 6, 7747.	12.8	1,336
53	Electronic structure evolution of fullerene on CH3NH3PbI3. Applied Physics Letters, 2015, 106, .	3.3	44
54	Scalable fabrication of efficient organolead trihalide perovskite solar cells with doctor-bladed active layers. Energy and Environmental Science, 2015, 8, 1544-1550.	30.8	606

#	Article	IF	CITATIONS
55	Surface analytical investigation on organometal triiodide perovskite. Journal of Vacuum Science and Technology B:Nanotechnology and Microelectronics, 2015, 33, .	1.2	43
56	Efficiency Enhancement in Polymer Solar Cells With a Polar Small Molecule Both at Interface and in the Bulk Heterojunction Layer. IEEE Journal of Photovoltaics, 2015, 5, 1408-1413.	2.5	5
57	Interfacial electronic structure at the CH3NH3PbI3/MoOx interface. Applied Physics Letters, 2015, 106, .	3.3	152
58	INDUCTION OF CYTOKINE PRODUCTION IN CHEETAH (ACINONYX JUBATUS) PERIPHERAL BLOOD MONONUCLEAR CELLS AND VALIDATION OF FELINE-SPECIFIC CYTOKINE ASSAYS FOR ANALYSIS OF CHEETAH SERUM. Journal of Zoo and Wildlife Medicine, 2015, 46, 306-313.	0.6	7
59	Giant switchable photovoltaic effect in organometal trihalide perovskite devices. Nature Materials, 2015, 14, 193-198.	27.5	1,372
60	Electronic structures at the interface between Au and CH ₃ NH ₃ PbI ₃ . Physical Chemistry Chemical Physics, 2015, 17, 896-902.	2.8	82
61	Engineering Crystalline Grain of Hybrid Perovskites for High Efficiency Solar Cells and Beyond. , 2015, ,		1
62	Transcriptome profiling of CTLs regulated by rapamycin using RNA-Seq. Immunogenetics, 2014, 66, 625-633.	2.4	11
63	Origin and elimination of photocurrent hysteresis by fullerene passivation in CH3NH3PbI3 planar heterojunction solar cells. Nature Communications, 2014, 5, 5784.	12.8	2,531
64	An Ultravioletâ€ŧoâ€NIR Broad Spectral Nanocomposite Photodetector with Gain. Advanced Optical Materials, 2014, 2, 549-554.	7.3	183
65	Arising applications of ferroelectric materials in photovoltaic devices. Journal of Materials Chemistry A, 2014, 2, 6027-6041.	10.3	408
66	Large Gain, Low Noise Nanocomposite Ultraviolet Photodetectors with a Linear Dynamic Range of 120 dB. Advanced Optical Materials, 2014, 2, 348-353.	7.3	84
67	Polymer aggregation correlated transition from Schottky-junction to bulk heterojunction organic solar cells. Applied Physics Letters, 2014, 104, 143304.	3.3	22
68	Efficient, high yield perovskite photovoltaic devices grown by interdiffusion of solution-processed precursor stacking layers. Energy and Environmental Science, 2014, 7, 2619-2623.	30.8	1,154
69	Large fill-factor bilayer iodine perovskite solar cells fabricated by a low-temperature solution-process. Energy and Environmental Science, 2014, 7, 2359-2365.	30.8	754
70	Solvent Annealing of Perovskiteâ€Induced Crystal Growth for Photovoltaicâ€Device Efficiency Enhancement. Advanced Materials, 2014, 26, 6503-6509.	21.0	1,527
71	Understanding the formation and evolution of interdiffusion grown organolead halide perovskite thin films by thermal annealing. Journal of Materials Chemistry A, 2014, 2, 18508-18514.	10.3	276
72	Universal Formation of Compositionally Graded Bulk Heterojunction for Efficiency Enhancement in Organic Photovoltaics. Advanced Materials, 2014, 26, 3068-3075.	21.0	139

#	Article	IF	CITATIONS
73	Alkylamine Assisted Ultrasound Exfoliation of MoS ₂ Nanosheets and Organic Photovoltaic Application. Nanoscience and Nanotechnology Letters, 2014, 6, 685-691.	0.4	8
74	Zinc alloyed iron pyrite ternary nanocrystals for band gap broadening. Journal of Materials Chemistry A, 2013, 1, 12060.	10.3	22
75	Synthesis and Application of Ferroelectric P(VDFâ€TrFE) Nanoparticles in Organic Photovoltaic Devices for High Efficiency. Advanced Energy Materials, 2013, 3, 1581-1588.	19.5	50
76	Fullerene Photodetectors with a Linear Dynamic Range of 90 dB Enabled by a Cross‣inkable Buffer Layer. Advanced Optical Materials, 2013, 1, 289-294.	7.3	127
77	4-(Methylnitrosamino)-1-(3-pyridyl)-1-butanone (NNK) regulates CTL activation and memory programming. Biochemical and Biophysical Research Communications, 2013, 435, 472-476.	2.1	3
78	Fluorine substituted thiophene–quinoxalinecopolymer to reduce the HOMO level and increase the dielectric constant for high open-circuit voltage organic solar cells. Journal of Materials Chemistry C, 2013, 1, 630-637.	5.5	101
79	Room-temperature organic ferromagnetism in the crystalline poly(3-hexylthiophene): Phenyl-C61-butyric acid methyl ester blend film. Polymer, 2013, 54, 490-494.	3.8	13
80	Wnt signaling inhibits CTL memory programming. Molecular Immunology, 2013, 56, 423-433.	2.2	7
81	TLR agonists are highly effective at eliciting functional memory CTLs of effector memory phenotype in peptide immunization. International Immunopharmacology, 2013, 15, 67-72.	3.8	25
82	Solutionâ€Processed Fullereneâ€Based Organic Schottky Junction Devices for Largeâ€Openâ€Circuitâ€Voltage Organic Solar Cells. Advanced Materials, 2013, 25, 572-577.	21.0	101
83	Biodegradable transparent substrates for flexible organic-light-emitting diodes. Energy and Environmental Science, 2013, 6, 2105.	30.8	281
84	Solution-Processed Fullerene-Based Organic Schottky Junction Devices for Large-Open-Circuit-Voltage Organic Solar Cells (Adv. Mater. 4/2013). Advanced Materials, 2013, 25, 571-571.	21.0	4
85	Ferroelectric Materials: Synthesis and Application of Ferroelectric P(VDFâ€TrFE) Nanoparticles in Organic Photovoltaic Devices for High Efficiency (Adv. Energy Mater. 12/2013). Advanced Energy Materials, 2013, 3, 1672-1672.	19.5	2
86	Nicotine Inhibits Memory CTL Programming. PLoS ONE, 2013, 8, e68183.	2.5	16
87	Cytotoxic T Lymphocytes and Vaccine Development 2013. BioMed Research International, 2013, 2013, 1-1.	1.9	0
88	Cholera toxin activates nonconventional adjuvant pathways that induce protective CD8 T-cell responses after epicutaneous vaccination. Proceedings of the National Academy of Sciences of the United States of America, 2012, 109, 2072-2077.	7.1	31
89	Understanding the effect of ferroelectric polarization on power conversion efficiency of organic photovoltaic devices. Energy and Environmental Science, 2012, 5, 8558.	30.8	64
90	A nanocomposite ultraviolet photodetector based on interfacial trap-controlled charge injection. Nature Nanotechnology, 2012, 7, 798-802.	31.5	634

#	Article	IF	CITATIONS
91	Utilizing insulating nanoparticles as the spacer in laminated flexible polymer solar cells for improved mechanical stability. Nanotechnology, 2012, 23, 344007.	2.6	10
92	Repetitive peptide boosting progressively enhances functional memory CTLs. Biochemical and Biophysical Research Communications, 2012, 424, 635-640.	2.1	4
93	Effect of Dietary Selenium and Cancer Cell Xenograft on Peripheral T and B Lymphocytes in Adult Nude Mice. Biological Trace Element Research, 2012, 146, 230-235.	3.5	12
94	Cytotoxic T Lymphocytes and Vaccine Development 2011. Journal of Biomedicine and Biotechnology, 2011, 2011, 1-1.	3.0	1
95	Temporal Regulation of Rapamycin on Memory CTL Programming by IL-12. PLoS ONE, 2011, 6, e25177.	2.5	17
96	Cytotoxic T Lymphocytes and Vaccine Development. Journal of Biomedicine and Biotechnology, 2010, 2010, 1-1.	3.0	0
97	Programming for CD8 T Cell Memory Development Requires IL-12 or Type I IFN. Journal of Immunology, 2009, 182, 2786-2794.	0.8	185
98	Species specialization in cytokine biology: Is interleukin-4 central to the TH1–TH2 paradigm in swine?. Developmental and Comparative Immunology, 2009, 33, 344-352.	2.3	56
99	The CD8 T cell response to vaccinia virus exhibits site-dependent heterogeneity of functional responses. International Immunology, 2007, 19, 733-743.	4.0	20
100	Detuning CD8 T cells: down-regulation of CD8 expression, tetramer binding, and response during CTL activation. Journal of Experimental Medicine, 2007, 204, 2667-2677.	8.5	119
101	Molecular basis for checkpoints in the CD8 T cell response: Tolerance versus activation. Seminars in Immunology, 2007, 19, 153-161.	5.6	38
102	Signals required for programming effector and memory development by CD8 + T cells. Immunological Reviews, 2006, 211, 81-92.	6.0	513
103	Î ³ Î [°] Lymphocyte Response to Porcine Reproductive and Respiratory Syndrome Virus. Viral Immunology, 2005, 18, 490-499.	1.3	40
104	The Level of Virus-Specific T-Cell and Macrophage Recruitment in Porcine Reproductive and Respiratory Syndrome Virus Infection in Pigs Is Independent of Virus Load. Journal of Virology, 2004, 78, 5923-5933.	3.4	164
105	β-Clucan enhancement of T cell IFNγ response in swine. Veterinary Immunology and Immunopathology, 2004, 102, 315-320.	1.2	77
106	Immunological Responses of Swine to Porcine Reproductive and Respiratory Syndrome Virus Infection. Viral Immunology, 2002, 15, 533-547.	1.3	252
107	CD4+ T Cell Responses to Pathogens in Cattle. , 0, , .		1